Atmos. Meas. Tech., 9, 3851–3861, 2016
www.atmos-meas-tech.net/9/3851/2016/
doi:10.5194/amt-9-3851-2016

Atmospheric Measurement Techniques
Open Access
EGU

A new technique for the direct detection of HO_2 radicals using bromide chemical ionization mass spectrometry (Br-CIMS): initial characterization

Javier Sanchez[1], David J. Tanner[2], Dexian Chen[2], L. Gregory Huey[2], and Nga L. Ng[1,2]

[1]School of Chemical and Biomolecular Engineering, Georgia Institute of Technology, Atlanta, GA 30332, USA
[2]School of Earth and Atmospheric Sciences, Georgia Institute of Technology, Atlanta, GA 30332, USA

Correspondence to: Nga L. Ng (ng@chbe.gatech.edu)

Received: 4 April 2016 – Published in Atmos. Meas. Tech. Discuss.: 6 April 2016
Revised: 21 July 2016 – Accepted: 22 July 2016 – Published: 19 August 2016

Abstract. Hydroperoxy radicals (HO_2) play an important part in tropospheric photochemistry, yet photochemical models do not capture ambient HO_2 mixing ratios consistently. This is likely due to a combination of uncharacterized chemical pathways and measurement limitations. The indirect nature of current HO_2 measurements introduces challenges in accurately measuring HO_2; therefore a direct technique would help constrain HO_x chemistry in the atmosphere. In this work we evaluate the feasibility of using chemical ionization mass spectrometry (CIMS) and propose a direct HO_2 detection scheme using bromide as a reagent ion. Ambient observations were made with a high-resolution time-of-flight chemical ionization mass spectrometer (HR-ToF-CIMS) in Atlanta over the month of June 2015 to demonstrate the capability of this direct measurement technique. Observations displayed expected diurnal profiles, reaching daytime median values of ~ 5 ppt between 2 and 3 p.m. local time. The HO_2 diurnal profile was found to be influenced by morning-time vehicular NO_x emissions and shows a slow decrease into the evening, likely from non-photolytic production, among other factors. Measurement sensitivities of approximately 5.1 ± 1.0 cps ppt^{-1} for a bromide ion ($^{79}Br^-$) count rate of 10^6 cps were observed. The relatively low instrument background allowed for a 3σ lower detection limit of 0.7 ppt for a 1 min integration time. Mass spectra of ambient measurements showed the $^{79}BrHO_2^-$ peak was the major component of the signal at nominal mass-to-charge 112, suggesting high selectivity for HO_2 at this mass-to-charge. More importantly, this demonstrates that these measurements can be achieved using instruments with only unit mass resolution capability.

1 Introduction

Hydroperoxy radicals (HO_2) play an important role in the photochemistry of the troposphere. They are primarily formed from the OH initiated oxidation of CO and other volatile organic compounds (VOCs), with contributions from ozonolysis of alkenes, nitrate radical oxidation of VOCs, and photolysis of aldehydes (e.g., HCHO) (Geyer et al., 2003; Cooke et al., 2010; Volkamer et al., 2010; Alam et al., 2013; Stone et al., 2014). HO_2 is a reservoir species for OH, the primary daytime oxidant, and facilitates the photochemical production of ozone via its reaction with NO. Additionally, the relative abundance of HO_2 to NO_x plays a critical role in the fate of peroxy radicals (RO_2) and the production of low-volatility products in secondary organic aerosol (SOA) formation (Orlando and Tyndall, 2012; Ziemann and Atkinson, 2012). For instance, reactions of HO_2 with RO_2 serve as the main source of atmospheric organic hydroperoxides, which are important constituents of SOA (Docherty et al., 2005).

HO_2 is also critical for the evaluation of model photochemical schemes. Because HO_2 is short lived (Heard and Pilling, 2003), HO_2 measurements allow for evaluation of model photochemistry with the exclusion of confounding phenomena, such as atmospheric transport. However, accurate measurements have proven difficult due to the naturally low abundance of HO_2. HO_2 also possess weak spectral lines, which has posed challenges for spectroscopic techniques. Nevertheless, some spectroscopic measurements have been made, primarily in the laboratory. Radford et al. (1974) employed laser magnetic resonance (LMR) spec-

troscopy in the laboratory to measure HO_2 while Mihelcic et al. (1985, 2003) used matrix isolation electron spin resonance (MIESR). The latter requires HO_2 to be collected for a period of 30 min on a D_2O matrix at 77 K before detection. Both techniques directly measure HO_2 but their applicability to atmospheric observations is limited, due to either instrumentation needs or low time resolution.

More recent methods such as peroxy radical chemical amplification (PERCA) (Cantrell and Stedman, 1982; Cantrell et al., 1984; Liu et al., 2009; Horstjann et al., 2014), chemical ionization mass spectrometry (CIMS) (Hanke et al., 2002; Edwards et al., 2003; Hornbrook et al., 2011; Kim et al., 2013; Wolfe et al., 2014), and laser induced fluorescence (LIF) (Stevens et al., 1994; Brune et al., 1995; Griffith et al., 2013; Walker et al., 2015) provide lower detection limits at high temporal resolution. However, these techniques do not measure HO_2 directly. Instead, the aforementioned techniques require that HO_2 be titrated with NO, which may introduce additional complexity, primarily from reactions of NO with RO_2. The PERCA technique, for example, exploits the radical chain reactions of HO_2 with NO and OH with CO to produce multiple NO_2 molecules from each HO_2 present in the sample. The production of NO_2 molecules is proportional to the contact time between the added reagents and the sample gas. Because multiple NO_2 molecules are produced from each HO_2, the signal is effectively amplified. The NO_2 has then traditionally been detected using luminol, though some recent measurements employ cavity ring-down spectroscopy (Liu et al., 2009; Horstjann et al., 2014). If organic peroxy radicals are present, the addition of NO to the sample gas results in additional production of HO_2; therefore the technique allows for the measurement of $HO_2 + RO_2$. As of yet, speciation of HO_2 from other peroxy radicals has not been successful, though previous attempts have been made (Miyazaki et al., 2010).

Chemical ionization techniques such as RO_x Chemical Conversion/CIMS (ROxMAS) (Hanke et al., 2002) and Peroxy radical CIMS (PerCIMS) (Edwards et al., 2003; Hornbrook et al., 2011; Kim et al., 2013; Wolfe et al., 2014) also rely on addition of NO to the sample gas. The OH produced from HO_2 titration subsequently reacts with SO_2 which is added to the inlet to produce H_2SO_4. The H_2SO_4 is then ionized by nitrate ions (NO_3^-) to produce a stable HSO_4^- product ion for detection. Because NO is added, PerCIMS suffers from positive artifacts from the contribution of the $RO_2 + NO$ reaction to the measured HO_2 concentration. Previous attempts to limit the contribution of the $RO_2 + NO$ reaction have been made. For example, Hornbrook et al. (2011) successfully speciated HO_2 and $HO_2 + RO_2$ measurements by modulating the relative NO and O_2 concentrations in the reaction region, suppressing the conversion of some peroxy radicals to ~ 15 %. However, the effectiveness of the oxygen dilution modulation scheme depends largely on the chemical structure of the hydrocarbons in the sample. Unsaturated hydrocarbons, such as isoprene, have additional pathways to the formation of HO_2 which are not suppressed by the oxygen dilution modulation scheme.

Unlike CIMS techniques and chemical amplification, the laser induced fluorescence technique does not require multiple conversion steps. It only requires the titration of HO_2 to OH, which is subsequently detected using laser excitation at 308 nm. The relative simplicity of the technique allows for more effective control of reaction time, which can be used to minimize $RO_2 + NO$ reactions. Nevertheless, LIF instruments have previously been shown to be susceptible to similar artifacts, with magnitudes dependent on the effective reaction time allowed after NO addition before detection and on peroxy radical precursor composition of the sample gas (Fuchs et al., 2011; Whalley et al., 2013).

Given the uncertainties associated with indirect methods of HO_2 measurement and the time resolution required for atmospheric measurements, a direct fast time resolution measurement of HO_2 would benefit efforts aiming to measure and model HO_2 in order to understand atmospheric photochemistry. The exclusion of measurement artifacts would aid in evaluating the gap between measured and modeled HO_2 concentrations in forested regions, where measured to modeled HO_2 ratios are highly variable (Stone et al., 2012). In this work, we evaluated the potential of various chemical ionization schemes and propose the Br^- ionization of HO_2 to form a $Br^-(HO_2)$ adduct as a direct method for measuring HO_2 using chemical ionization mass spectrometry. This technique provides selective, fast time resolution measurements of HO_2. Ambient measurements were conducted in Atlanta in June 2015 to demonstrate instrument performance. Important measurement considerations and future improvements are also discussed.

2 Instrument description

A high-resolution time-of-flight chemical ionization mass spectrometer (HR-ToF-CIMS, Aerodyne Research, Inc.) and a house-built quadrupole CIMS were used for laboratory characterizations of reagent ions for the measurement of HO_2. Ambient data were collected using the HR-ToF-CIMS exclusively. The HR-ToF-CIMS consists of an atmospheric pressure interface with five differentially pumped stages, utilizing two scroll pumps and a multi-stage turbomolecular pump. The instrument design has been described in detail by Bertram et al. (2011). Figure 1 shows a schematic diagram of the HR-ToF-CIMS. HO_2 is measured by introducing 2 standard L min^{-1} of sample into the ion–molecule reaction region through a 0.5 mm orifice and mixed with Br^- reagent produced by passing 10 sccm of a 0.2 % CF_3Br / N_2 mixture carried by ~ 2 standard L min^{-1} N_2 gas (99.999 %, Airgas) through a cylindrical 10 mCi ^{210}Po alpha radiation source. The ion–molecule reaction region (IMR) has a residence time of 0.07 s and is operated at a pressure of 100 mbar. The contents of the IMR were sub-sampled through a 0.3 mm critical orifice leading to the instrument's ion optics. HO_2 present

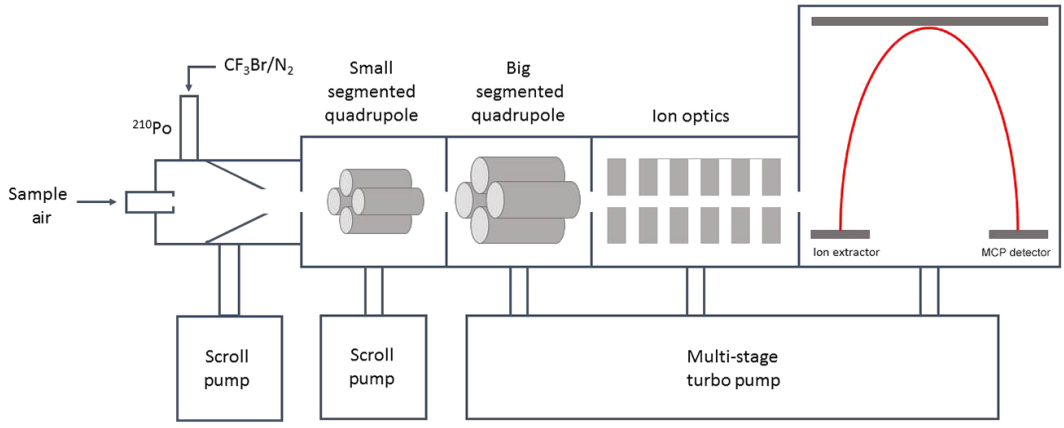

Figure 1. Schematic diagram of the high-resolution time-of-flight chemical ionization mass spectrometer (HR-ToF-CIMS). Sample air enters the ion–molecule reaction region through a 0.5 mm orifice where it is ionized at 100 mbar. The contents of the ion–molecule reaction region are sub-sampled through a 0.3 mm orifice into the small segmented quadrupole (SSQ) chamber held at 2.5 mbar. Collisional dissociation occurs in the SSQ. Ion products are then collimated by the big segmented quadrupole (BSQ) where they also dissipate energy by collisions with background gas at reduced pressure. The subsequent ion lenses then focus and accelerate the ion beam towards the ToF analyzer.

in the sample cluster with Br^- to form $Br^-(HO_2)$ adducts which are transmitted by a series of ion optics and speciated by the time-of-flight spectrometer. The isotopic abundance of bromine is such that the adduct is detected at two nominal mass-to-charge ratios, m/z 112 and m/z 114 corresponding to the ^{79}Br and ^{81}Br isotopes, respectively. The adducts have fractional mass-to-charge ratios of 111.9165 and 113.9144 Th. In order to demonstrate the generalizability of the technique to instruments with unit mass resolution, only the unit mass resolution data are used for ambient measurements, though the high-resolution capabilities were exploited to diagnose and address possible artifacts during the method development. The high-resolution mass spectra are also used to unambiguously identify the $BrHO_2^-$ adducts. In contrast to the HR-ToF-CIMS, the quadrupole CIMS was operated at an ion–molecule reaction region pressure of 15 torr. The sample and N_2 flow rates were both 2 standard L min^{-1}.

3 HO_2 generation and calibration procedure

HO_2 were generated for the evaluation of chemical ionization schemes and instrument calibrations by water photolysis at 184.9 nm using a mercury UV lamp as previously described by a number of studies e.g., (Tanner et al., 1997; Holland et al., 2003; Smith et al., 2006; Dusanter et al. 2008). Air was humidified by passing the gas stream through glass bubblers and diluted in dry air from a pure air generator (AADCO 747-14) to vary the relative humidity of the gas. The gas stream was then introduced into a black anodized aluminum square flow tube (15.6 mm × 15.6 mm × 520 mm) and exposed to UV radiation through a small slit. HO_2 concentrations were calculated using Eq. (1),

$$\Delta[HO_2] = \phi\sigma I[H_2O]\Delta t, \quad (1)$$

where ϕ, σ, I, and Δt represent the quantum yield, water absorption cross-section, UV lamp photon flux at 184.9 nm, and irradiation time, respectively. The quantum yield was assumed to be unity and a value of 7.22×10^{-20} cm^2 was used for the water absorption cross section (Creasey et al., 2000). The lamp photon flux was measured using a Hamamatsu Phototube (Hamamatsu Photonics), and found to be 2.6×10^{13} photons cm^{-2} s^{-1}. A bandpass filter (HORIBA Scientific) was used to selectively transmit at 185 nm. The dew point of the gas was measured using a LICOR LI-840A CO_2 / H_2O gas analyzer. The irradiation time was calculated based on the flow velocity which was measured using a Dwyer pitot tube and a magnehelic pressure sensor. Flow velocities varied between 400 and 800 cm s^{-1} ($Re > 4000$) to promote plug flow conditions. The slit allowing light into the tube was located such that the distance before irradiation after entry into the tube was 10 times the hydraulic diameter, allowing the flow profile to fully develop before exposure to UV light. Plug flow conditions were confirmed by measuring the flow velocity both at the center line and near the wall of the tube, showing no measurable differences. The water vapor mixing ratios varied between 0.66 and 8.20 ppt. The time after irradiation before introduction into the instrument was minimized ($\tau \sim 60$ ms) to avoid additional HO_2 generation from OH oxidation of trace CO present in the N_2 gas. It was calculated that less than 8 % of the OH formed would react with CO to produce additional HO_2 assuming a CO concentration of 500 ppb. Addition of 40 ppm of C_3F_6 as an OH scavenger had no effect on the HO_2 signal intensity, confirming the lack of contribution from OH oxidation to HO_2 production. The HO_2 concentration was kept low (2–45 ppt) to calibrate for the HO_2 levels observed during ambient sampling and to avoid non-linearity in the calibration curve due to depletion of HO_2 through HO_2 radical–radical recombi-

nation. At the HO_2 mixing ratios employed, less than 1 % of HO_2 are estimated to be lost to recombination. The overall calibration uncertainty is 18 % (1σ). The contribution of the different parameters to the overall uncertainty is given in Table S1 in the Supplement. A conservative estimate of 20 % is used in this work.

4 Laboratory characterizations and reagent ion selection

Prior to the selection of Br^- for our ionization scheme, a number of negative reagent ions were evaluated for their ability to detect HO_2. HO_2 were generated using the procedure in Sect. 3. HO_2 mixing ratios were typically in excess of 300 ppt for initial reagent ion evaluation, and varied by varying the gas humidity and velocity. NO was added in excess (2–4 ppm) to obtain the instrument background. NO was also added in small concentrations and in increasing increments to roughly test the kinetics suggested by the HO_2 signal response to additions of varying concentrations of NO, as additional confirmation that the analyte being observed corresponded to HO_2. Tests were conducted primarily at room temperature (293 K). The humidity of the gas stream was determined by the amount of water vapor added to produce HO_2. No additional sources of water vapor were present, nor was water directly added to the IMR. The reagent ions evaluated included O_2^-, SF_6^-, Cl^-, and I^-. Because of their low electron affinities, O_2^- and SF_6^- were utilized in an attempt to produce the HO_2^- ion directly via charge exchange. However, HO_2^- was not observed in laboratory characterization experiments. It is likely that the HO_2^- ion formed but was not detected due to its low electron affinity (Ramond et al., 2002), which results in high reactivity. The SF_6^- ionization did yield a cluster at mass-to-charge 52, which was assigned as HO_2F^- in the high-resolution mass spectrum. However, the signal was not quantitatively reproducible and did not remain constant for a given HO_2 concentration. Additionally, the form of the cluster is more likely to be O_2^-(HF) than $F^-(HO_2)$ (Seeley et al., 1996), which may compromise the selectivity of the measurement, as O_2^- ions are not uniquely formed from the ionization of HO_2.

Chloride and iodide reagent ions were generated from HCl and CH_3I mixtures, respectively. Full mass spectra obtained using the quadrupole CIMS identified Cl^-(HCl), $Cl^-(HNO_3)$, and $Cl^-(CF_3COOH)$ as prominent ions. However, the $Cl^-(HO_2)$ cluster was not observed. The characterizations involving chloride reagent ions in the laboratory were conducted using the quadrupole CIMS. Unlike the other ions, which were evaluated with the HR-ToF-CIMS as well as the quadrupole CIMS, Cl^- was not revisited with the HR-ToF-CIMS instrument.

The I^- reagent ion, which has been used extensively to measure both organic and inorganic species (Huey et al., 1995; Slusher et al., 2004; Lee et al., 2014; Woodward-Massey et al., 2014; Brophy and Farmer, 2015; Faxon et al., 2015; Nah et al., 2016; Lee et al., 2016), was found to cluster with HO_2, appearing at mass-to-charge 160, consistent with observations by Veres et al. (2015). However, we observed that addition of NO_2 (Scott-Marrin, 100 ppm v/v N_2) to a clean N_2 gas matrix resulted in an increase of 1 cps per ppb NO_2 per 10^6 cps I^- in the m/z 160 signal. A 20 ppb addition results in a 20 cps increase in the m/z 160 signal, equivalent to $\sim$ 4 ppt of HO_2. The addition of NO_2 showed an increase in a peak (m/z 159.9896) not associated with HO_2 that we could not identify. The addition of NO_2 did not affect the high-resolution $I^-(HO_2)$ signal but is expected to be a significant artifact for instruments of low resolving power.

Unlike the other reagent ions, the Br^- ionization scheme was found to be sensitive to HO_2, the measurements were reproducible, and there were no observed positive artifacts from NO_2 or O_3, making this an ideal scheme for measurements of HO_2. To evaluate potential positive artifacts as observed using iodide, NO_2 was added to the N_2 gas sample and measured using the bromide reagent, but no increase in the $Br^-(HO_2)$ (nominal m/z 112 and m/z 114) signals was observed. Parts per million mixing ratios of ozone were also introduced into the inlet in a clean N_2 matrix but did not cause any changes in the Br^- (HO_2) cluster signal. While Br^- has the disadvantage of having a $\sim$ 50 % natural isotopic abundance with nominal m/z 79 and 81, HO_2 calibrations performed as described in Sect. 4 showed similar absolute sensitivities for the $I^-(HO_2)$ and $^{79}Br^-(HO_2)$ clusters using I^- and Br^- reagents, respectively. A synthesized mixture containing primarily ^{79}Br could nearly double the sensitivity at the m/z 112 cluster if necessary, giving Br^- a potential advantage over I^- with respect to sensitivity. The $^{79}Br^-(HO_2)$ cluster was used preferentially over the $^{81}Br^-(HO_2)$ cluster for ambient data because m/z 114 has a contribution from the isotope of a large m/z 113 CF_3COO^- signal which arises from impurities in PFA Teflon™. Iodide ionization was attempted once more during ambient sampling, which will be discussed in Sect. 5.3.

Br^- ionization: sensitivity, selectivity, humidity, and temperature dependence

The instrument sensitivity using Br^- reagent was calibrated following the procedure in Sect. 3. Figure 2 shows HO_2 calibration curves for $^{79}Br^-(HO_2)$ at m/z 112. The figure shows two separate calibrations performed on two different occasions to illustrate reproducibility. The curves are linear with slopes of 4.95 ± 1.00 and 5.26 ± 1.05 which represent the instrument sensitivity in cps ppt^{-1} for a $^{79}Br^-$ ion count of 10^6 cps. Intercepts of 27 ± 5 and 30 ± 3 are observed for the calibration curves which are not explained by errors in any of the parameters used to calculate the expected HO_2 concentrations in Eq. (1). Instead, there appears to be a constant HO_2 photolytic source independent of water photolysis. The unidentified source requires the presence of water vapor but

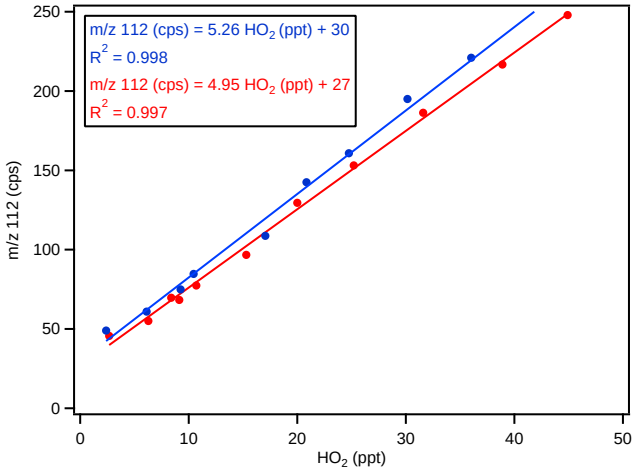

Figure 2. Laboratory HO_2 calibration curves for the $^{79}Br^-(HO_2)$ cluster as observed at nominal m/z 112. The slopes represent the sensitivity in cps ppt^{-1}. HO_2 mixing ratios are calculated using Eq. (1). Two calibrations conducted on separate occasions are shown to illustrate reproducibility. The error associated with the individual sensitivities is 20 % which arises from the combined uncertainty of the calibration parameters (Eq. 1).

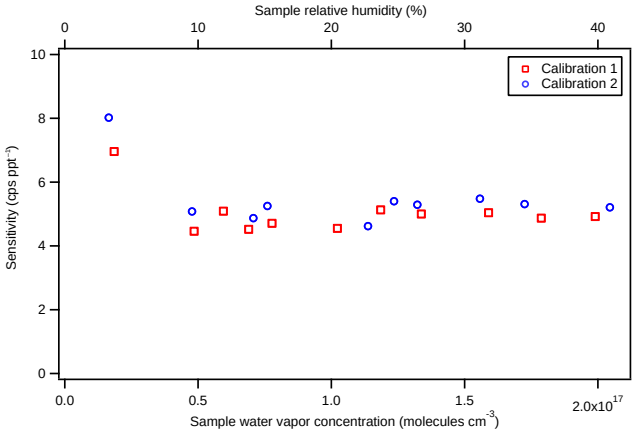

Figure 3. Instrument sensitivity as measured at m/z 112 ($^{79}Br^-(HO_2)$) as a function of sample relative humidity. The instrument sensitivity demonstrates no water vapor dependence beyond a sample relative humidity of 10 %. The "Calibration 1" and "Calibration 2" labels refer to the curves in Fig. 2.

does not scale with the absolute water vapor mixing ratio. Further, addition of 40 ppm C_3F_6 as OH scavenger did not have an effect on the observed intercept, suggesting that the HO_2 production is unrelated to OH oxidation. The magnitude of the HO_2 formation from this unknown source scales linearly with the UV lamp flux. The intercept does not affect the sensitivity and is not used to calculate the HO_2 mixing ratio. The uncertainty in the sensitivity is derived from the combined uncertainties of the parameters used in Eq. (1), as well as random error in the HO_2 signal, resulting in a 1σ uncertainty of 20 %. Contributions to the overall uncertainty for each parameter are listed in Table S1. The time series of one HO_2 calibration at both m/z 112 and 114 are shown in Fig. S2 in the Supplement to illustrate the rapid instrument response to varying levels of analyte.

The $Br^-(HO_2)$ measurement selectivity was explored further in the laboratory. In addition to high concentration additions of NO_2 and O_3, other common atmospheric constituents were sampled with the instrument to assess the possibility of other potential artifacts. Large concentrations (> 10 ppm) of SO_2 were added, which did not elicit a response. Hydrogen peroxide and formaldehyde were sampled from the Georgia Tech Environmental Chamber facility (Boyd et al., 2015) at concentrations in excess of several ppm, eliciting responses of 0.25 and 0.002 cps ppb^{-1} at m/z 112, respectively. It is not clear whether the observed signal response is due to ion–molecule reaction with Br^- or unidentified wall reactions within the experimental chamber. Regardless, these responses are insignificant under most atmospheric and laboratory experimental conditions. Furthermore, if the resulting signal increase is due to reactions inside the IMR, the contribution of these species can be removed from the measurement by obtaining appropriate instrument backgrounds, such as by using additions of NO. Such additions would remove HO_2 in the sample, but not remove H_2O_2 or HCHO. The small contributions to the signal at m/z 112 would be present in the background and therefore removed from the measurement.

Another important consideration for this technique is the effect of temperature and humidity on cluster stability, which was explored during laboratory characterizations. The effect of varying water vapor mixing ratios in the sample gas on sensitivity is shown in Fig. 3. At relative humidities in the sample below 10 %, the sensitivity appears to have a strong, negative water dependence. However, when the humidity in the sample gas is higher than 10 %, the sensitivity is invariant with increasing relative humidity, which simplifies ambient sampling, as no humidity-dependent correction is required. The temperature dependence was also explored, where an IMR temperature increase from 20 to 40 °C resulted in a 20 % decrease in instrument sensitivity. The relatively strong negative temperature dependence suggests that $Br^-(HO_2)$ is a weak cluster. This highlights the importance of temperature control and performing calibrations at the sampling temperature.

5 Ambient measurements

To demonstrate the applicability of the Br^- ionization scheme to ambient HO_2 measurements, a field study was conducted in June 2015 (9–25 June 2015) in Atlanta at an urban site located on the roof (30–40 m above ground) of the Ford Environmental Science & Technology building on the Georgia Tech campus, which has been used for previous ambient studies (Hennigan et al., 2008; Xu et al., 2015a, b). The

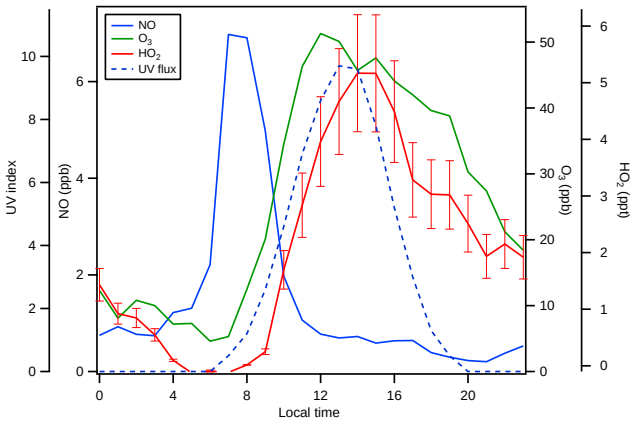

Figure 4. Hourly median diurnal profiles of HO_2, NO, O_3 and UV index in Atlanta. The sampling period was during 9 June 2015 21:14:00 to 11 June 2015 13:28:00, and 15 June 2015 01:52:00 to 25 June 2015 01:32:00 LT.

site is about 840 m west of Interstate 75/85 and can therefore be affected by traffic emissions. The instrument was located outside in an enclosure, allowing for a short 1 cm inner diameter Teflon™ inlet of approximately 13 cm in length. The residence time of ambient sample in the tube was short (0.3 s) which helps to minimize HO_2 surface losses on the sample tubing. Data was collected at a 1 Hz frequency and averaged to 1 min. A solenoid valve was used to perform periodic additions of 10 sccm of an NO / N_2 mixture (Scott-Marrin, 810 ppm) into the sample stream every 10 min on a 10 % duty cycle to obtain the measurement background. The m/z 112 signal was normalized to a $^{79}Br^-$ count of 10^6 cps to account for temporal changes in reagent ion abundance.

Various co-located instruments were deployed for simultaneous measurements of O_3, NO, NO_2, and HNO_4. NO concentrations were measured using a Teledyne 200EU chemiluminescence monitor while NO_2 was measured by a Cavity Attenuated Phase Shift NO_2 monitor (Aerodyne Research, Inc.). Ozone was measured using a Teledyne Model T400 UV absorption analyzer. Pernitric acid (HNO_4), formed from the reaction of HO_2 with NO_2 was also monitored using a house-built quadruple CIMS with an iodide-adduct ionization scheme and observed at m/z 206. A similar configuration of the instrument has been described previously by Slusher et al. (2004). Previous measurements of HNO_4 using I^- have been conducted by Veres et al. (2015). Meteorological data, including temperature and humidity, were recorded using a Vantage Pro2 weather station. An additional UV sensor was employed with the Vantage Pro2 weather station to obtain an UV index measurement between 280 and 360 nm.

5.1 Bromide-CIMS measurements of HO_2

Figure 4 shows the diurnal profiles of HO_2, as well as the diurnal profiles of the UV radiation index, NO, and O_3 concentrations. The difference in the time between peak actinic flux and peak HO_2 concentration is at least partially due to the suppression of HO_2 by the presence of NO from morning-time traffic emissions. The HO_2 rises once the NO concentration is sufficiently low and peaks between 2 and 3 p.m. with a mixing ratio of $\sim$ 5 ppt, comparable to previous studies in other urban regions (Emmerson et al., 2005; Kanaya et al., 2007; Dusanter et al., 2009). The 3σ limit of detection was calculated to be 0.7 ppt for a 1 min integration time based on laboratory calibrations and baselines observed during ambient sampling, which is sufficiently low for atmospherically important HO_2 concentrations. The slow decay of HO_2 in early evening may partially be explained by non-photolytic HO_2 production, e.g., from oxidation of biogenic volatile organic compounds (BVOCs), which are abundant in the Southeast United States (Geron et al., 2000; Guenther et al., 2006), as well as a decrease in boundary layer height. However, additional measurements would be required to constrain sources and sinks.

The mass spectrum for a 24 h period of ambient observations is shown in Fig. 5 and compared to a laboratory spectrum generated during HO_2 calibration. Few additional peaks are present in ambient spectrum, suggesting that Br^- ionization is selective at the mass-to-charge values shown in the figure. Further, the majority of the additional peaks have signal intensities much lower than the intensity of the HO_2 signal at m/z 112, which makes it unlikely that the species at the additional peaks and their respective isotopes will affect the signal at m/z 112.

HNO_4 and NO_2 measurements were used to infer HO_2 concentration for comparison with the measured HO_2 concentrations. The HNO_4 and HO_2 are assumed to be in thermal equilibrium for the calculation. Details regarding the calculation are discussed in the Supplement. Their respective diurnal profiles are shown in Fig. S3. The profiles agree well temporally but not quantitatively, differing by a factor of 5 during the afternoon. A more complete discussion regarding the comparison is presented in the Supplement.

5.2 Instrument background determinations

Measurement backgrounds were conducted by the addition of NO to the sample gas, as mentioned previously. To evaluate the accuracy of the instrument background, a metal wool scrubber was utilized for comparison to the NO addition. The scrubber was first tested to ensure complete scrubbing of sample HO_2 by generation of additional HO_2 in ambient air with a mercury lamp. Though HO_2 was generated, none was observed when the scrubber was placed before the instrument, demonstrating that the scrubber was effectively removing all HO_2 in the sample gas.

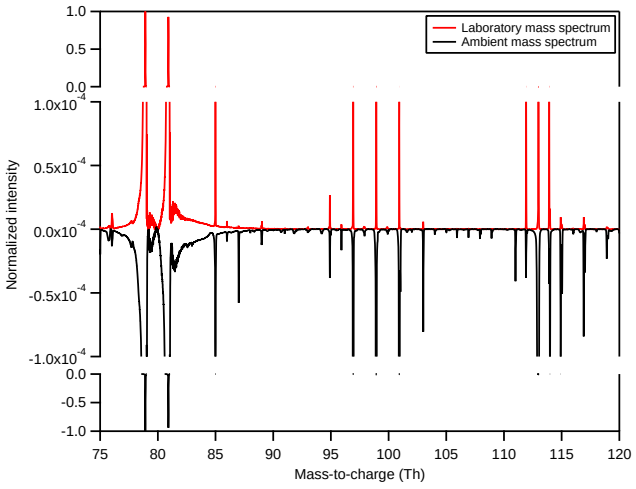

Figure 5. Comparison of laboratory generated and ambient mass spectra. Laboratory data was collected during HO_2 calibration using the procedure described in Sect. 3. Ambient data from a 24 h period during ambient sampling is shown here. The ambient mass spectrum is reversed for clarity. Few additional peaks are observed in the ambient spectrum, the majority of which are of low signal intensity. Prominent known peaks are at m/z 79 and 81 (Br^-), m/z 85 (CF_3O^-), m/z 97 ($^{79}Br^-(H_2O)$), m/z 99 ($^{81}Br^-(H_2O)$ and $^{79}Br^-(HF)$), m/z 101 ($^{81}Br^-(HF)$), and m/z 113 (CF_3COO^-).

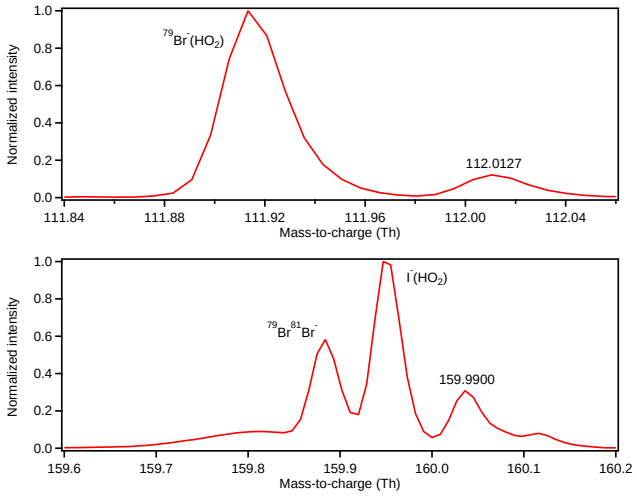

Figure 6. Normalized high-resolution mass spectra of nominal m/z 112 for the Br^- ionization of HO_2 (top panel) and m/z 160 for the I^- ionization of HO_2 (bottom panel). The $^{79}Br^{81}Br^-$ peak corresponds to Br_2 added directly to the sample flow from a permeation tube as an additional calibrant.

It was observed that the two methods of obtaining the instrument background did not agree, with the NO addition providing a lower background signal than the metal wool scrubber. Furthermore, additions of NO to the sample air after physical scrubbing further decreased the HO_2 signal. This suggests that there is internal HO_2 generation within the instrument. Laboratory characterizations were conducted to explore the discrepancy. In the laboratory, adding NO to a clean N_2 sample matrix also decreased the observed HO_2 background signal. The differences in HO_2 backgrounds observed between the different backgrounding methods and NO additions to N_2 gas were similar, representing ~ 4 ppt of HO_2 generated inside the instrument. The similarity suggests that HO_2 generation is independent of sample composition. The HO_2 is likely produced from ion-molecule reactions of trace gases in the N_2 used for ion generation. The HO_2 mixing ratios were corrected by subtraction of an additional, constant 4 ppt contribution from internal HO_2 generation.

Based on the observations made in this work, future instrument backgrounds can be conducted in alternative ways to eliminate the need for post-correction. For example, a physical scrubber may be used as has been done here to avoid removal of internally generated HO_2 from the background signal. Alternatively, the NO addition concentration and contact time can be optimized such that the $HO_2 + NO$ reaction is efficient in the sample line before the instrument, where the pressure is approximately atmospheric, but inefficient inside the IMR, where the pressure is at least a factor of 10 lower. The addition of NO under optimal conditions would then only titrate HO_2 efficiently in the sample line, but would not allow significant NO reaction with internally generated HO_2.

5.3 Iodide-CIMS measurements of HO_2

Despite artifacts observed in the measurements of laboratory-generated HO_2, iodide ionization measurements were conducted during a short ambient sampling period (25 July 2015 06:00 p.m. to 27 July 2015 10:00 a.m.) to assess its viability in a real air matrix for the measurement of HO_2. We observed that the measured $I^-(HO_2)$ signals were not consistent with the expected behavior of HO_2. The time series did not show a clear diurnal pattern, nor was the signal effectively suppressed by NO additions. Instead, NO additions caused m/z 160 to increase. The high-resolution capability of the HR-ToF-CIMS allowed for the peak assignment of $I^-(HO_2)$ with high accuracy but the time series of the high-resolution peak displayed a similar behavior to that of the low resolution data. The resolving power of the instrument during the sampling period was ~ 3000 and the high-resolution time series of the major peaks at nominal m/z 160 appear to be mostly independent of each other, which suggests that resolution is not a limiting factor. Additionally, a peak (m/z 159.990 Th) which may pertain to the NO_2 related artifact observed during earlier laboratory characterizations was present (Fig. 6). Because the sampling period was short, the possibility of using iodide for HO_2 measurements may warrant further exploration. However, our laboratory and ambient measurements suggest that for iodide to be viable, high-resolution capability will

be necessary for accurate measurements due to artifacts caused by the presence of NO_2. This is not the case for Br^-. Figure 6 shows the mass spectra of Br^- and I^- at the mass-to-charge ratios where the HO_2 clusters are observed. The Br^- spectrum shows that the $Br^-(HO_2)$ cluster is the dominant species at m/z 112. The minor peak observed is always present and does not vary significantly over the course of the day. Furthermore, the peak does not respond to NO additions, making NO backgrounds effective at eliminating any contribution to the signal from this peak. Thus, the measurement of HO_2 with Br^- does not require high-resolution capability.

6 Conclusions and future work

HO_2 is an important contributor to photochemistry in the atmosphere. In this work, we investigated the feasibility of a direct chemical ionization measurement of HO_2. We evaluated a number of negative reagent ions (O_2^-, SF_6^-, Cl^-, I^-, and Br^-) using a HR-ToF-CIMS and found that detection of HO_2 using charge exchange ionization is not feasible in the real atmosphere. However, ionization of HO_2 via clustering was found to be a promising mechanism for the direct measurement of atmospheric HO_2. Among the reagent ions evaluated, Br^- was found to be the best candidate for the measurement of HO_2, providing improved selectivity over I^-. The HO_2 sensitivities as measured at m/z 160 and m/z 112 using iodide and bromide, respectively, were found to be similar, giving Br^- a potential advantage in sensitivity, as an isotopically pure $CF_3^{79}Br$ mixture should nearly double the sensitivity at m/z 112. Using Br^- also allows for the measurement of HO_2 at a lower m/z which may decrease the likelihood of measurement interferences and reduce ambiguity in peak identification, as a smaller number of possible chemical formulas for ion products are possible. Furthermore, Br has a high electron affinity, which makes the production of small charged ions from ionization and collisional dissociation unlikely.

Ambient measurements were conducted in Atlanta in June 2015 to demonstrate the performance and capability of the instrument. The sensitivity using Br^- (5.1 ± 1.00 cps ppt^{-1} per 10^6 ^{79}Br ion counts) was sufficient for ground-based measurements as the observed baselines were relatively low. Furthermore, the absolute sensitivity for HO_2 may also be significantly improved by using a radioactive source with higher activity, provided that measures are taken to suppress the increased background due to internal HO_2 generation. The measured HO_2 diurnal profile behaves in a manner consistent with the NO_x and HNO_4 abundance, though there exist no previous measurements for HO_2 in Atlanta available for a more quantitative comparison. Future work will focus on optimizing the instrument sensitivity to HO_2, conducting instrument intercomparisons, and further exploring Br^- ionization for the measurement of other atmospherically important species.

7 Data availability

The data presented in this paper are available upon request from the corresponding author.

The Supplement related to this article is available online at doi:10.5194/amt-9-3851-2016-supplement.

Acknowledgements. This work was supported by National Science Foundation grant 1455588. The HR-ToF-CIMS was purchased with NSF Major Research Instrumentation (MRI) grant 1428738. J. Sanchez acknowledges support by the NASA Earth and Space Science Fellowship (NESSF) and the Alfred P. Sloan Minority Ph.D. (MPHD) Scholarship. D. Chen, L. Huey, and D. Tanner were supported by NSF grant #1262033. The authors would like to thank Wing Y. Tuet for helpful comments.

Edited by: A. Hofzumahaus
Reviewed by: two anonymous referees

References

Alam, M. S., Rickard, A. R., Camredon, M., Wyche, K. P., Carr, T., Hornsby, K. E., Monks, P. S., and Bloss, W. J.: Radical Product Yields from the Ozonolysis of Short Chain Alkenes under Atmospheric Boundary Layer Conditions, J. Phys. Chem. A, 117, 12468–12483, doi:10.1021/jp408745h, 2013.

Bertram, T. H., Kimmel, J. R., Crisp, T. A., Ryder, O. S., Yatavelli, R. L. N., Thornton, J. A., Cubison, M. J., Gonin, M., and Worsnop, D. R.: A field-deployable, chemical ionization time-of-flight mass spectrometer, Atmos. Meas. Tech., 4, 1471–1479, doi:10.5194/amt-4-1471-2011, 2011.

Boyd, C. M., Sanchez, J., Xu, L., Eugene, A. J., Nah, T., Tuet, W. Y., Guzman, M. I., and Ng, N. L.: Secondary organic aerosol formation from the β-pinene+NO_3 system: effect of humidity and peroxy radical fate, Atmos. Chem. Phys., 15, 7497–7522, doi:10.5194/acp-15-7497-2015, 2015.

Brophy, P. and Farmer, D. K.: A switchable reagent ion high resolution time-of-flight chemical ionization mass spectrometer for real-time measurement of gas phase oxidized species: characterization from the 2013 southern oxidant and aerosol study, Atmos. Meas. Tech., 8, 2945–2959, doi:10.5194/amt-8-2945-2015, 2015.

Brune, W. H., Stevens, P. S., and Mather, J. H.: Measuring OH and HO_2 in the troposphere by laser-induced fluorescence at low-pressure, J. Atmos. Sci., 52, 3328–3336, doi:10.1175/1520-0469(1995)052<3328:moahit>2.0.co;2, 1995.

Cantrell, C. A. and Stedman, D. H.: A possible technique for the measurement of atmospheric peroxy radicals, Geophys. Res. Lett., 9, 846–849, doi:10.1029/GL009i008p00846, 1982.

Cantrell, C. A., Stedman, D. H., and Wendel, G. J.: Measurement of Atmospheric Peroxy-Radicals by Chemical Amplification, Anal. Chem., 56, 1496–1502, doi:10.1021/Ac00272a065, 1984.

Cooke, M. C., Utembe, S. R., Carbajo, P. G., Archibald, A. T., Orr-Ewing, A. J., Jenkin, M. E., Derwent, R. G., Lary, D. J., and Shallcross, D. E.: Impacts of formaldehyde photolysis rates on tropospheric chemistry, Atmos. Sci. Lett., 11, 33–38, doi:10.1002/asl.251, 2010.

Creasey, D. J., Heard, D. E., and Lee, J. D.: Absorption cross-section measurements of water vapour and oxygen at 185 nm. Implications for the calibration of field instruments to measure OH, HO_2 and RO_2 radicals, Geophys. Res. Lett., 27, 1651–1654, doi:10.1029/1999GL011014, 2000.

Docherty, K. S., Wu, W., Lim, Y. B., and Ziemann, P. J.: Contributions of Organic Peroxides to Secondary Aerosol Formed from Reactions of Monoterpenes with O_3, Environ. Sci. Technol., 39, 4049–4059, doi:10.1021/es050228s, 2005.

Dusanter, S., Vimal, D., and Stevens, P. S.: Technical note: Measuring tropospheric OH and HO_2 by laser-induced fluorescence at low pressure. A comparison of calibration techniques, Atmos. Chem. Phys., 8, 321–340, doi:10.5194/acp-8-321-2008, 2008.

Dusanter, S., Vimal, D., Stevens, P. S., Volkamer, R., and Molina, L. T.: Measurements of OH and HO_2 concentrations during the MCMA-2006 field campaign – Part 1: Deployment of the Indiana University laser-induced fluorescence instrument, Atmos. Chem. Phys., 9, 1665–1685, doi:10.5194/acp-9-1665-2009, 2009.

Edwards, G. D., Cantrell, C. A., Stephens, S., Hill, B., Goyea, O., Shetter, R. E., Mauldin, R. L., Kosciuch, E., Tanner, D. J., and Eisele, F. L.: Chemical ionization mass spectrometer instrument for the measurement of tropospheric HO_2 and RO_2, Anal. Chem., 75, 5317–5327, doi:10.1021/Ac034402b, 2003.

Emmerson, K. M., Carslaw, N., Carpenter, L. J., Heard, D. E., Lee, J. D., and Pilling, M. J.: Urban Atmospheric Chemistry During the PUMA Campaign 1: Comparison of Modelled OH and HO_2 Concentrations with Measurements, J. Atmos. Chem., 52, 143–164, doi:10.1007/s10874-005-1322-3, 2005.

Faxon, C. B., Bean, J. K., and Ruiz, L. H.: Inland Concentrations of Cl-2 and $ClNO_2$ in Southeast Texas Suggest Chlorine Chemistry Significantly Contributes to Atmospheric Reactivity, Atmosphere-Basel, 6, 1487–1506, doi:10.3390/atmos6101487, 2015.

Fuchs, H., Bohn, B., Hofzumahaus, A., Holland, F., Lu, K. D., Nehr, S., Rohrer, F., and Wahner, A.: Detection of HO_2 by laser-induced fluorescence: calibration and interferences from RO_2 radicals, Atmos. Meas. Tech., 4, 1209–1225, doi:10.5194/amt-4-1209-2011, 2011.

Geron, C., Rasmussen, R., Arnts, R. R., and Guenther, A.: A review and synthesis of monoterpene speciation from forests in the United States, Atmos. Environ., 34, 1761–1781, doi:10.1016/S1352-2310(99)00364-7, 2000.

Geyer, A., Bachmann, K., Hofzumahaus, A., Holland, F., Konrad, S., Klupfel, T., Patz, H. W., Perner, D., Mihelcic, D., Schafer, H. J., Volz-Thomas, A., and Platt, U.: Nighttime formation of peroxy and hydroxyl radicals during the BERLIOZ campaign: Observations and modeling studies, J. Geophys. Res.-Atmos., 108, 8249, doi:10.1029/2001jd000656, 2003.

Griffith, S. M., Hansen, R. F., Dusanter, S., Stevens, P. S., Alaghmand, M., Bertman, S. B., Carroll, M. A., Erickson, M., Galloway, M., Grossberg, N., Hottle, J., Hou, J., Jobson, B. T., Kammrath, A., Keutsch, F. N., Lefer, B. L., Mielke, L. H., O'Brien, A., Shepson, P. B., Thurlow, M., Wallace, W., Zhang, N., and Zhou, X. L.: OH and HO_2 radical chemistry during PROPHET 2008 and CABINEX 2009 – Part 1: Measurements and model comparison, Atmos. Chem. Phys., 13, 5403–5423, doi:10.5194/acp-13-5403-2013, 2013.

Guenther, A., Karl, T., Harley, P., Wiedinmyer, C., Palmer, P. I., and Geron, C.: Estimates of global terrestrial isoprene emissions using MEGAN (Model of Emissions of Gases and Aerosols from Nature), Atmos. Chem. Phys., 6, 3181–3210, doi:10.5194/acp-6-3181-2006, 2006.

Hanke, M., Uecker, J., Reiner, T., and Arnold, F.: Atmospheric peroxy radicals: ROXMAS, a new mass-spectrometric methodology for speciated measurements of HO_2 and Sigma RO_2 and first results, Int. J. Mass. Spectrom., 213, 91–99, doi:10.1016/S1387-3806(01)00548-6, 2002.

Heard, D. E. and Pilling, M. J.: Measurement of OH and HO_2 in the Troposphere, Chem. Rev., 103, 5163–5198, doi:10.1021/cr020522s, 2003.

Hennigan, C. J., Bergin, M. H., Dibb, J. E., and Weber, R. J.: Enhanced secondary organic aerosol formation due to water uptake by fine particles, Geophys. Res. Lett., 35, L18801, doi:10.1029/2008GL035046, 2008.

Holland, F., Hofzumahaus, A., Schäfer, J., Kraus, A., and Pätz, H.-W.: Measurements of OH and HO_2 radical concentrations and photolysis frequencies during BERLIOZ, J. Geophys. Res.-Atmos., 108, PHO 2-1–PHO 2-23, doi:10.1029/2001JD001393, 2003.

Hornbrook, R. S., Crawford, J. H., Edwards, G. D., Goyea, O., Mauldin III, R. L., Olson, J. S., and Cantrell, C. A.: Measurements of tropospheric HO_2 and RO_2 by oxygen dilution modulation and chemical ionization mass spectrometry, Atmos. Meas. Tech., 4, 735–756, doi:10.5194/amt-4-735-2011, 2011.

Horstjann, M., Andrés Hernández, M. D., Nenakhov, V., Chrobry, A., and Burrows, J. P.: Peroxy radical detection for airborne atmospheric measurements using absorption spectroscopy of NO_2, Atmos. Meas. Tech., 7, 1245–1257, doi:10.5194/amt-7-1245-2014, 2014.

Huey, L. G., Hanson, D. R., and Howard, C. J.: Reactions of SF6− and I− with Atmospheric Trace Gases, J. Phys. Chem., 99, 5001–5008, doi:10.1021/j100014a021, 1995.

Kanaya, Y., Cao, R., Akimoto, H., Fukuda, M., Komazaki, Y., Yokouchi, Y., Koike, M., Tanimoto, H., Takegawa, N., and Kondo, Y.: Urban photochemistry in central Tokyo: 1. Observed and modeled OH and HO_2 radical concentrations during the winter and summer of 2004, J. Geophys. Res.-Atmos., 112, D21312, doi:10.1029/2007JD008670, 2007.

Kim, S., Wolfe, G. M., Mauldin, L., Cantrell, C., Guenther, A., Karl, T., Turnipseed, A., Greenberg, J., Hall, S. R., Ullmann, K., Apel, E., Hornbrook, R., Kajii, Y., Nakashima, Y., Keutsch, F. N., DiGangi, J. P., Henry, S. B., Kaser, L., Schnitzhofer, R., Graus, M., Hansel, A., Zheng, W., and Flocke, F. F.: Evaluation of HO_x sources and cycling using measurement-constrained model calculations in a 2-methyl-3-butene-2-ol (MBO) and monoterpene (MT) dominated ecosystem, Atmos. Chem. Phys., 13, 2031–2044, doi:10.5194/acp-13-2031-2013, 2013.

Lee, B. H., Lopez-Hilfiker, F. D., Mohr, C., Kurten, T., Worsnop, D. R., and Thornton, J. A.: An Iodide-Adduct High-Resolution Time-of-Flight Chemical-Ionization Mass Spectrometer: Application to Atmospheric Inorganic and Organic Compounds, Environ. Sci. Technol., 48, 6309–6317, doi:10.1021/es500362a, 2014.

Lee, B. H., Mohr, C., Lopez-Hilfiker, F. D., Lutz, A., Hallquist, M., Lee, L., Romer, P., Cohen, R. C., Iyer, S., Kurtén, T., Hu, W., Day, D. A., Campuzano-Jost, P., Jimenez, J. L., Xu, L., Ng, N. L., Guo, H., Weber, R. J., Wild, R. J., Brown, S. S., Koss, A., de Gouw, J., Olson, K., Goldstein, A. H., Seco, R., Kim, S., McAvey, K., Shepson, P. B., Starn, T., Baumann, K., Edgerton, E. S., Liu, J., Shilling, J. E., Miller, D. O., Brune, W., Schobesberger, S., D'Ambro, E. L., and Thornton, J. A.: Highly functionalized organic nitrates in the southeast United States: Contribution to secondary organic aerosol and reactive nitrogen budgets, P. Natl. Acad. Sci. USA, 113, 1516–1521, doi:10.1073/pnas.1508108113, 2016.

Liu, Y., Morales-Cueto, R., Hargrove, J., Medina, D., and Zhang, J.: Measurements of Peroxy Radicals Using Chemical Amplification-Cavity Ringdown Spectroscopy, Environ. Sci. Technol., 43, 7791–7796, doi:10.1021/es901146t, 2009.

Mihelcic, D., Müsgen, P., and Ehhalt, D. H.: An improved method of measuring tropospheric NO_2 and RO_2 by matrix isolation and electron spin resonance, J. Atmos. Chem., 3, 341–361, doi:10.1007/BF00122523, 1985.

Mihelcic, D., Holland, F., Hofzumahaus, A., Hoppe, L., Konrad, S., Müsgen, P., Pätz, H. W., Schäfer, H. J., Schmitz, T., Volz-Thomas, A., Bächmann, K., Schlomski, S., Platt, U., Geyer, A., Alicke, B., and Moortgat, G. K.: Peroxy radicals during BERLIOZ at Pabstthum: Measurements, radical budgets and ozone production, J. Geophys. Res.-Atmos., 108, 8254, doi:10.1029/2001JD001014, 2003.

Miyazaki, K., Parker, A. E., Fittschen, C., Monks, P. S., and Kajii, Y.: A new technique for the selective measurement of atmospheric peroxy radical concentrations of HO_2 and RO_2 using a denuding method, Atmos. Meas. Tech., 3, 1547–1554, doi:10.5194/amt-3-1547-2010, 2010.

Nah, T., Sanchez, J., Boyd, C. M., and Ng, N. L.: Photochemical Aging of α-pinene and β-pinene Secondary Organic Aerosol formed from Nitrate Radical Oxidation, Environ. Sci. Technol., 50, 222–231, doi:10.1021/acs.est.5b04594, 2016.

Orlando, J. J. and Tyndall, G. S.: Laboratory studies of organic peroxy radical chemistry: an overview with emphasis on recent issues of atmospheric significance, Chem. Soc. Rev., 41, 6294–6317, doi:10.1039/C2CS35166H, 2012.

Radford, H. E., Evenson, K. M., and Howard, C. J.: HO_2 detected by laser magnetic resonance, J. Chem. Phys., 60, 3178–3183, doi:10.1063/1.1681503, 1974.

Ramond, T. M., Blanksby, S. J., Kato, S., Bierbaum, V. M., Davico, G. E., Schwartz, R. L., Lineberger, W. C., and Ellison, G. B.: Heat of Formation of the Hydroperoxyl Radical HOO Via Negative Ion Studies, J. Phys. Chemi. A, 106, 9641–9647, doi:10.1021/jp014614h, 2002.

Seeley, J. V., Meads, R. F., Elrod, M. J., and Molina, M. J.: Temperature and Pressure Dependence of the Rate Constant for the $HO_2 + NO$ Reaction, J. Phys. Chem., 100, 4026–4031, doi:10.1021/jp952553f, 1996.

Slusher, D. L., Huey, L. G., Tanner, D. J., Flocke, F. M., and Roberts, J. M.: A thermal dissociation–chemical ionization mass spectrometry (TD-CIMS) technique for the simultaneous measurement of peroxyacyl nitrates and dinitrogen pentoxide, J. Geophys.l Res.-Atmos., 109, D19315, doi:10.1029/2004JD004670, 2004.

Smith, S. C., Lee, J. D., Bloss, W. J., Johnson, G. P., Ingham, T., and Heard, D. E.: Concentrations of OH and HO_2 radicals during NAMBLEX: measurements and steady state analysis, Atmos. Chem. Phys., 6, 1435–1453, doi:10.5194/acp-6-1435-2006, 2006.

Stevens, P. S., Mather, J. H., and Brune, W. H.: Measurement of tropospheric OH and HO_2 by laser-induced fluorescence at low-pressurE, J. Geophys. Res.-Atmos., 99, 3543–3557, doi:10.1029/93jd03342, 1994.

Stone, D., Whalley, L. K., and Heard, D. E.: Tropospheric OH and HO_2 radicals: field measurements and model comparisons, Chem. Soc. Rev., 41, 6348–6404, doi:10.1039/C2CS35140D, 2012.

Stone, D., Evans, M. J., Walker, H., Ingham, T., Vaughan, S., Ouyang, B., Kennedy, O. J., McLeod, M. W., Jones, R. L., Hopkins, J., Punjabi, S., Lidster, R., Hamilton, J. F., Lee, J. D., Lewis, A. C., Carpenter, L. J., Forster, G., Oram, D. E., Reeves, C. E., Bauguitte, S., Morgan, W., Coe, H., Aruffo, E., Dari-Salisburgo, C., Giammaria, F., Di Carlo, P., and Heard, D. E.: Radical chemistry at night: comparisons between observed and modelled HO_x, NO_3 and N_2O_5 during the RONOCO project, Atmos. Chem. Phys., 14, 1299–1321, doi:10.5194/acp-14-1299-2014, 2014.

Tanner, D. J., Jefferson, A., and Eisele, F. L.: Selected ion chemical ionization mass spectrometric measurement of OH, J. Geophys. Res.-Atmos., 102, 6415–6425, doi:10.1029/96JD03919, 1997.

Veres, P. R., Roberts, J. M., Wild, R. J., Edwards, P. M., Brown, S. S., Bates, T. S., Quinn, P. K., Johnson, J. E., Zamora, R. J., and de Gouw, J.: Peroxynitric acid (HO_2NO_2) measurements during the UBWOS 2013 and 2014 studies using iodide ion chemical ionization mass spectrometry, Atmos. Chem. Phys., 15, 8101–8114, doi:10.5194/acp-15-8101-2015, 2015.

Volkamer, R., Sheehy, P., Molina, L. T., and Molina, M. J.: Oxidative capacity of the Mexico City atmosphere – Part 1: A radical source perspective, Atmos. Chem. Phys., 10, 6969–6991, doi:10.5194/acp-10-6969-2010, 2010.

Walker, H. M., Stone, D., Ingham, T., Vaughan, S., Cain, M., Jones, R. L., Kennedy, O. J., McLeod, M., Ouyang, B., Pyle, J., Bauguitte, S., Bandy, B., Forster, G., Evans, M. J., Hamilton, J. F., Hopkins, J. R., Lee, J. D., Lewis, A. C., Lidster, R. T., Punjabi, S., Morgan, W. T., and Heard, D. E.: Night-time measurements of HO_x during the RONOCO project and analysis of the sources of HO_2, Atmos. Chem. Phys., 15, 8179–8200, doi:10.5194/acp-15-8179-2015, 2015.

Whalley, L. K., Blitz, M. A., Desservettaz, M., Seakins, P. W., and Heard, D. E.: Reporting the sensitivity of laser-induced fluorescence instruments used for HO_2 detection to an interference from RO_2 radicals and introducing a novel approach that enables HO_2 and certain RO_2 types to be selectively measured, Atmos. Meas. Tech., 6, 3425–3440, doi:10.5194/amt-6-3425-2013, 2013.

Wolfe, G. M., Cantrell, C., Kim, S., Mauldin III, R. L., Karl, T., Harley, P., Turnipseed, A., Zheng, W., Flocke, F., Apel, E. C., Hornbrook, R. S., Hall, S. R., Ullmann, K., Henry, S. B., DiGangi, J. P., Boyle, E. S., Kaser, L., Schnitzhofer, R., Hansel, A., Graus, M., Nakashima, Y., Kajii, Y., Guenther, A., and Keutsch, F. N.: Missing peroxy radical sources within a summertime ponderosa pine forest, Atmos. Chem. Phys., 14, 4715–4732, doi:10.5194/acp-14-4715-2014, 2014.

Woodward-Massey, R., Taha, Y. M., Moussa, S. G., and Osthoff, H. D.: Comparison of negative-ion proton-transfer with iodide

ion chemical ionization mass spectrometry for quantification of isocyanic acid in ambient air, Atmos. Environ., 98, 693–703, doi:10.1016/j.atmosenv.2014.09.014, 2014.

Xu, L., Guo, H., Boyd, C. M., Klein, M., Bougiatioti, A., Cerully, K. M., Hite, J. R., Isaacman-VanWertz, G., Kreisberg, N. M., Knote, C., Olson, K., Koss, A., Goldstein, A. H., Hering, S. V., de Gouw, J., Baumann, K., Lee, S.-H., Nenes, A., Weber, R. J., and Ng, N. L.: Effects of anthropogenic emissions on aerosol formation from isoprene and monoterpenes in the southeastern United States, P. Natl. Acad. Sci., 112, 37–42, doi:10.1073/pnas.1417609112, 2015a.

Xu, L., Suresh, S., Guo, H., Weber, R. J., and Ng, N. L.: Aerosol characterization over the southeastern United States using high-resolution aerosol mass spectrometry: spatial and seasonal variation of aerosol composition and sources with a focus on organic nitrates, Atmos. Chem. Phys., 15, 7307–7336, doi:10.5194/acp-15-7307-2015, 2015b.

Ziemann, P. J. and Atkinson, R.: Kinetics, products, and mechanisms of secondary organic aerosol formation, Chem. Soc. Rev., 41, 6582–6605, doi:10.1039/C2CS35122F, 2012.